Experimental Study on Sulfate Wetting–Drying Cycle of Metal Tailings Powder Concrete

Ruidong Wu[1,2], Min Zou[1,2], Juanhong Liu[1,2]*, Guangtian Zhang[1,2,3] and Yueyue Zhang[1,2]

[1]College of Civil and Resource Engineering, University of Science and Technology Beijing, Beijing, China, [2]Beijing Key Laboratory of Urban Underground Space Engineering, University of Science and Technology Beijing, Beijing, China, [3]Hebei Academy of Building Research, Shijiazhuang, China

In order to absorb a large amount of metal tailings powder and alleviate the shortage of mineral admixture in concrete, metal tailings powder can form a compound admixture with slag powder to prepare concrete. The sulfate wetting–drying cycle test of concrete with different contents of metal tailings powder was carried out to study the action law of metal tailings powder on the sulfate corrosion resistance of concrete. Scanning electron microscope, XRD, and nuclear magnetic resonance microscopic tests were used to reveal the deterioration mechanism of metal tailings powder concrete eroded by sulfate. The results show that proper addition of metal tailings powder can increase the sulfate corrosion resistance of C50 concrete. When the ratio of metal tailings powder to slag powder is 3:7 and 5:5, the sulfate corrosion resistance grade can reach KS180. There is a strong linear relationship between the relative ultrasonic velocity factor and relative compressive strength factor. The sulfate failure mechanism of metal tailings powder concrete is mainly the internal formation of corrosion products ettringite and gypsum. The introduction of metal tailings powder can reduce the alkalinity of concrete and improve the pore structure, thus improving the sulfate corrosion resistance of concrete.

Keywords: metal tailings, sulfate, wetting–drying cycle, micro powder, durability

INTRODUCTION

With the continuous development of economy and society, the mining volume of metal ore increases year by year. A large amount of tailings will be produced in the process of metal ore beneficiation. Most of the tailings will be stacked in the tailings pond after centralized discharge (Lvu et al., 2018; Huang et al., 2021; Zhao et al., 2021). Different from nonmetallic ores, there are many tailings produced by mineral processing of nonferrous ores, and the mining and stripping quality ratio of nonferrous ores is mostly between 1:2 and 1:14 (Yang and Guo, 2018).

According to statistics, there are about 70 billion tons of tailings stockpile in China (Yao et al., 2021), and the utilization rate of tailings is relatively low, resulting in the increase of mine solid waste stockpile year by year. A large number of tailings are accumulated in the tailings pond, which not only occupies a large amount of land and pollutes the surface environment but is also one of the major hazard sources, which seriously threatens the surrounding environment and safety. At present, tailings are mainly used for mine backfilling (Liu et al., 2017; Qi and Fourie, 2019; Wu et al., 2014), soil reclamation, preparation of building materials (Ullah et al., 2021), and preparation of new functional materials such as molecular sieve (Zhang et al., 2019; Yang et al., 2021). With the continuous development of beneficiation technology, tailings have become finer and finer. The stock

TABLE 1 | Property indexes of reference cement.

Fineness, mm	Water requirement of normal consistency, %	Setting time, min		Compressive strength, MPa		Flexural strength, MPa		Stability
		Initial	Final	3d	28d	3d	28d	
0.5	27.2	155	215	28.3	53.2	5.5	10.3	Qualified

of fine-grained tailings below 75 μm accumulates rapidly (Wu et al., 2020). Fine-grained tailings will cause a series of problems such as filling rheology and high cost (Zhang et al., 2021; Chen et al., 2022). The reuse of fine-grained tailings is difficult, and the utilization rate is very low (Wu et al., 2018), resulting in the comprehensive utilization rate of tailings being far lower than the new output of tailings; in particular, the industrialized utilization of fine-grained tailings needs to be solved urgently.

Continuous investment in infrastructure increases concrete consumption. High-quality mineral admixtures such as fly ash and slag powder are indispensable components of modern high-performance concrete. There is a shortage of high-quality mineral admixtures in some areas. Thermal power generation is gradually replaced, and the content of fly ash is bound to decline year by year. Therefore, it is imperative to find new admixtures for preparing concrete. The fine particles of metal tailings mainly take SiO_2 and Al_2O_3 as the main chemical components. The fine powder of metal tailings can be used as concrete admixture, which can not only alleviate the shortage of high-quality concrete admixture but also absorb a large number of fine-grained tailings. Han et al. (2017, 2019) believed that the hydration reaction of metal tailings powder in cement-based materials is slow. Wu et al. (2021) found that a small part of iron tailings powder can undergo hydration reaction after a long period. Hou et al. (2019) and Liu et al. (2019) found that the strength of metal tailings powder concrete increases with the increase of fineness. Lu et al. (2021) considered that the curing method has a great impact on the iron tailings micro powder concrete. Song et al. (2017), Song et al. (2019), and Song and Chen (2020) found that tailings powder can replace fly ash to prepare concrete. Research on the composite admixture of metal tailings mainly focuses on the mechanical properties and hydration process (Li et al., 2021; Zhang et al., 2021), and there are few studies on the impact of metal tailings powder on the durability of concrete, especially the research on the sulfate wetting–drying cycle of metal tailings powder concrete. The durability of concrete determines the service time of concrete. In order to realize the resource utilization of metal tailings powder in concrete, the influence law and action mechanism of tailings on the durability of concrete have to be studied. In this paper, the effect of metal tailings powder on the sulfate wetting–drying cyclic corrosion resistance of concrete is studied. The deterioration mechanism of metal tailings powder concrete in sulfate is revealed through micro analysis such as scanning electron microscope (SEM) and X-ray diffraction (XRD), which lays a theoretical foundation for the large-scale application of metal tailings powder concrete in a sulfate environment.

EXPERIMENTAL PROCEDURES

Raw Material

In order to avoid the influence of admixtures in cement on the test, P.I.42.5 pure Portland cement is adopted, and its properties are shown in **Table 1**. The mineral composition of cement is C_3S (59.6%), C_2S (19.5%), C_3A (7.2%), and C_4AF (8.3%).

The micro powder of metal tailings comes from a copper zinc mine in Fujian, China. It is fine-grained tailings screened by drying (45 μm sieve residue is 6.45%). The main component of tailings is SiO_2, as well as some chemical components such as iron, aluminum, copper, and zinc. An S95-grade slag is selected as slag powder, and its main components are SiO_2, CaO, Al_2O_3, etc. See **Tables 2**, **3** for specific technical indexes and the chemical composition of metal tailings powder and slag powder.

The coarse and fine aggregates used in the experiment are natural aggregates, and the indexes meet the national standards, as shown in **Table 4**.

Polycarboxylic acid superplasticizer is used as the admixture, with a solid content of about 20%.

Tap water is used for concrete mixing, and the chemical composition in tap water contains very little chloride ion, which will not affect the corrosion test.

Concrete Mix Proportion

In order to explore the action law of metal tailings powder on the sulfate resistance of concrete, the compound admixture of metal tailings powder and slag powder is adopted. The proportion of metal tailings powder in the compound admixture is 0%, 30%, 50%, 70%, and 100%. Two kinds of common concrete, C30 and C50, are prepared. Based on the consideration of low carbon and environmental protection, a low cement clinker and low water binder ratio system are adopted. The cement in C30 concrete is only 30% of the cementitious material, and the basic water binder ratio is 0.40. The cement in C50 concrete is 40% of the cementitious material, and the basic water binder ratio is 0.29. Because it is a low cement clinker system, through trial mixing, the basic water binder ratio is slightly lower than that of ordinary concrete. The water binder ratio of concrete decreases with the increase of the content of nonactive admixture, metal tailings powder, so as to ensure that the strength can meet the design grade. The specific proportion is shown in **Table 5**.

Experimental Procedures

Place the test piece (100 mm × 100 mm × 100 mm) standard curing for 26 days, take it out of the standard curing room, put it into the drying oven, and dry it at (80 ± 5)°C for 48 h. Take it out after drying, cool it to room temperature, and put the test block into a sulfate wetting–drying cycle test chamber. Prepare 5%

TABLE 2 | Technical indexes of metal tailings powder and slag powder.

	Density, g·cm^{-3}	Specific surface area, m^2·kg^{-1}	45 μm sieve residue, %	Water requirement ratio, %
Metal tailings	2.82	450	6.45	90
Slag	2.80	485	6.20	96.2

TABLE 3 | Main chemical components of metal tailings powder (%).

Chemical composition	SiO$_2$	CaO	Fe$_2$O$_3$	Al$_2$O$_3$	MgO	CuO	ZnO
Metal tailings	67.55	4.23	9.86	8.69	1.24	0.31	0.21
Slag	52.12	38.11	0.43	8.18	1.03	-	-

TABLE 4 | Technical indexes of coarse and aggregate.

	Apparent density, kg·m^{-3}	Bulk density, kg·m^{-3}	Porosity, %	Mud content, %	Crushing index, %	Needle and flake content, %	Fineness modulus
Coarse	2,743	1,569	42.8	1.0	5.2	5.5	-
Fine	2,595	1,534	39.0	1.6	-	-	2.7

TABLE 5 | Mix proportion of metal tailings powder concrete (kg/m^{-3}).

	Cement	Metal tailings powder	Slag powder	Sand	Stone	Water	W/B	PC
C30-0	113	0	264	840	1,018	151	0.40	3.4
C30-30	113	79	185			147	0.39	
C30-50	113	132	132			143	0.38	
C30-70	113	185	79			140	0.37	
C30-100	113	264	0			136	0.36	
C50-0	191	0	287	725	1,071	139	0.29	6.7
C50-30	191	86	201			134	0.28	
C50-50	191	144	144			129	0.27	
C50-70	191	201	86			124	0.26	
C50-100	191	287	0			119	0.25	

Na$_2$SO$_4$ solution as corrosion solution, and replace the sulfate solution every other month. The wetting–drying cycle is 24 h, including soaking for 16 h, drying for 6 h at a drying temperature of 80°C, and cooling for 2 h. The sulfate wetting–drying cycle experiment equipment is a NELD-LSC automatic sulfate wetting–drying cycle test machine. The concrete quality, ultrasonic velocity, and compressive strength of concrete were tested every 30 wetting–drying cycles. When the compressive strength of the concrete decreased to 75% before the test, it was regarded as sulfate erosion failure, and the test was stopped.

RESULTS AND DISCUSSION

Test Index Results of Concrete Sulfate Wetting–Drying Cycle

The sulfate wetting–drying cycle experiment of concrete with different mix proportions was carried out to compare the concrete quality, ultrasonic velocity, and compressive strength after different wetting–drying cycles, so as to study the influence of different metal tailings powder content on the sulfate corrosion resistance.

The relative compressive strength factor P is defined and calculated as follows:

$$P = \frac{P_i - P_0}{P_0} \times 100\% \qquad (1)$$

P is the relative intensity factor; P_0 is the compressive strength of the test piece before sulfate wetting–drying cycle, MPa. P_i is the compressive strength of the test piece after the ith cycle sulfate wetting–drying, MPa. The compressive strength of each group is tested after different sulfate wetting–drying cycles, as shown in **Figure 1**. The relative compressive strength factor is calculated, and the results are shown in **Table 6**.

In practice, testing the compressive strength needs to consume a large number of test blocks and cannot reflect

FIGURE 1 | Compressive strength of concrete after different wetting–drying cycles.
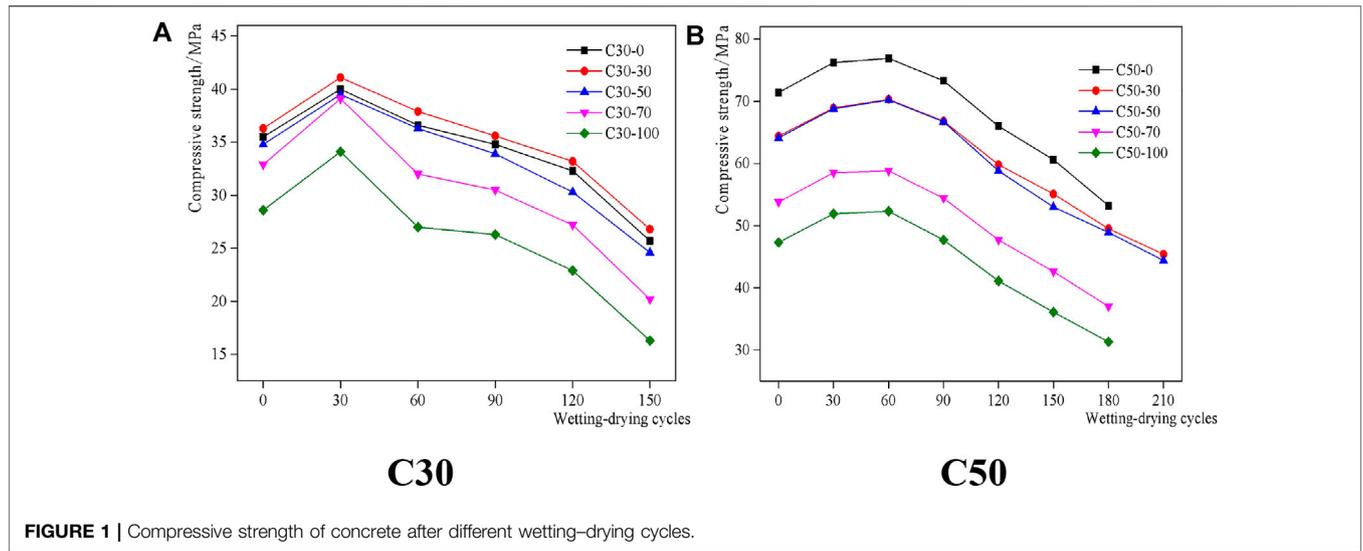
TABLE 6 | Relative compressive strength factor of concrete after sulfate wetting–drying cycles.

	30c	60c	90c	120c	150c	180c	210c
C30-0	12.6	3.1	−2.1	−8.9	**−27.7**		
C30-30	13.1	4.5	−1.8	−8.5	**−26.1**		
C30-50	13.5	4.2	−2.4	−12.8	**−29.3**		
C30-70	18.8	−2.7	−7.3	−17.2	**−38.5**		
C30-100	19.2	−5.6	−8.2	−19.9	**−43.1**		
C50-0	6.7	7.8	2.6	−7.6	−15.1	**−25.5**	
C50-30	7.1	9.1	3.8	−7.1	-14.5	−23.1	**−29.5**
C50-50	7.3	9.5	4.1	−8.2	−17.3	−23.6	**−30.8**
C50-70	8.8	9.3	1.2	−11.3	−20.8	**−31.2**	
C50-100	9.7	10.5	0.9	−13.2	−23.6	**−33.9**	

The bold value means that the sulfate failure condition is reached.

TABLE 7 | Relative mass factor of concrete after sulfate wetting–drying cycles.

	30c	60c	90c	120c	150c	180c	210c
C30-0	5.12	11.23	3.67	−2.22	**−6.20**		
C30-30	6.34	13.72	4.15	−2.83	**−5.72**		
C30-50	9.43	16.31	7.88	−1.43	**−3.13**		
C30-70	10.76	17.87	3.31	−4.49	**−10.28**		
C30-100	14.31	19.12	2.25	−6.66	**−13.12**		
C50-0	2.55	6.74	3.33	1.18	−0.67	**−2.03**	
C50-30	2.72	6.90	3.26	1.21	−0.55	−2.61	**−4.05**
C50-50	3.75	7.58	4.39	2.25	1.11	0.07	**−1.17**
C50-70	4.84	9.05	3.55	0.42	−1.84	**−5.67**	
C50-100	5.88	10.71	3.81	0.15	−3.71	**−8.92**	

The bold value means that the sulfate failure condition is reached.

TABLE 8 | Relative ultrasonic velocity factor of concrete after sulfate wetting–drying cycles.

	30c	60c	90c	120c	150c	180c	210c
C30-0	5.21	1.36	−0.88	−3.72	**−11.83**		
C30-30	5.52	1.90	−0.75	−3.58	**−10.88**		
C30-50	5.81	2.25	−1.02	−5.51	**−12.34**		
C30-70	8.13	−1.10	−3.08	−7.25	**−16.12**		
C30-100	8.45	−3.65	−3.56	−8.43	**−18.13**		
C50-0	2.76	3.25	1.21	−3.29	−6.29	**−10.76**	
C50-30	2.91	3.84	1.59	−3.06	−5.99	−9.63	**−12.29**
C50-50	3.08	4.08	1.75	−3.51	−7.33	−9.83	**−13.01**
C50-70	3.71	3.93	0.55	−4.78	−8.81	**−13.12**	
C50-100	4.15	4.46	0.38	−5.61	−9.95	**−14.28**	

The bold value means that the sulfate failure condition is reached.

M is the relative quality factor, M_0 is the mass of the test piece before the sulfate wetting–drying cycle, g. M_i is the mass of the test piece after the ith sulfate wetting–drying cycle, g. Test the mass of each group concrete after different sulfate wetting-drying cycles, and calculate the relative quality factor. The results are shown in **Table 7**.

The relative ultrasonic velocity factor V is defined, and the calculation formula is as follows:

$$V = \frac{V_i - V_0}{V_0} \times 100\% \qquad (3)$$

V is the relative wave velocity factor, V_0 is the ultrasonic velocity of the test piece before the sulfate wetting–drying cycle, m/s; V_i is the ultrasonic velocity of the test piece after the ith sulfate wetting–drying cycle, m/s. Test the ultrasonic velocity of each group concrete after different sulfate wetting–drying cycles, and calculate the relative ultrasonic velocity factor. The results are shown in **Table 8**.

The relative quality factor, relative ultrasonic velocity factor, and relative compressive strength factor of concrete specimens first increase and then decrease with the increase of sulfate dry

the sulfate corrosion process of concrete in structural service. Therefore, some nondestructive testing indicators such as quality and ultrasonic velocity should be developed. The relative quality factor M is defined and calculated as follows:

$$M = \frac{m_i - m_0}{m_0} \times 100\% \qquad (2)$$

FIGURE 2 | Picture of concrete specimen damaged by sulfate wetting–drying cycles.

and wet corrosion cycles. At the initial stage of corrosion, sodium sulfate solution continuously enters the concrete block through the pores. These sodium sulfate react with calcium hydroxide in the concrete to generate ettringite, gypsum, and other erosion products. In addition, the sodium sulfate solution continuously crystallizes inside, and these substances fill the small pores in the concrete. Therefore, the quality of the block has increased compared with that before corrosion, the interior is more dense, the ultrasonic velocity increases, and the compressive strength continues to improve. With the continuous advancement of the sulfate corrosion process, more and more ettringite, gypsum, and sodium sulfate crystals continue to accumulate in the concrete. Compared with the original hydration products, the expansion rate of these products increases, resulting in the continuous increase of internal volume, and micro cracks slowly occur in the concrete block. These micro cracks continue to expand and extend, resulting in the peeling off of the skin around the block, as shown in **Figure 2**. The relative quality factor, relative ultrasonic velocity factor, and relative compressive strength factor of concrete are reduced. When the expansion stress produced by erosion products is greater than the internal tensile strength of concrete, the micro cracks develop to the degree of penetration, and the concrete is corroded.

According to the standard, when the compressive strength decreases to 75% of the initial strength before corrosion, it is regarded as sulfate corrosion failure. The sulfate corrosion resistance grade of C30-0 to C30-100 groups is KS120. The sulfate resistance grade of C50-0, C50-70, and C50-100 groups is KS150, while the sulfate resistance grade of concrete with 30% and 50% of metal tailings powder accounting for mineral admixtures is KS180, which shows that the appropriate amount of metal tailings powder can improve the sulfate resistance of concrete, which is obvious in the C50 concrete. Taking C30-30 and C50-30 groups, in which the content of metal tailings powder accounts for 30% of mineral admixtures, as an example, the mass, ultrasonic velocity, and compressive strength

are the smallest, and the sulfate corrosion resistance is relatively strong.

Relationship Between Three Corrosion Deterioration Factors

As the indicator of sulfate corrosion in the national standard is compressive strength, but in the actual test process, the compressive strength test requires a large number of concrete blocks, it is difficult to test the accurate compressive strength in the actual application of a typical environment. Nondestructive corrosion factors such as ultrasonic velocity are an important supplement to the study of metal tailings powder concrete sulfate resistance. The three corrosion indexes of relative quality factor, relative ultrasonic velocity factor, and relative compressive strength factor have been defined earlier, and the relative relationship of the three corrosion factors has been established. See **Figure 3** to study the internal relationship and mutual characterization law of the three corrosion factors.

It can be seen from the above figure that the correspondence between the relative quality factor, the relative ultrasonic velocity factor, and the relative compressive strength factor is not obvious, so the change of the quality cannot reflect the change of the compressive strength after a certain number of wetting–drying cycles. The change of quality slightly lags behind the change of ultrasonic wave velocity and compressive strength. This is because the expansion, falling off, and filling are carried out together, and fine falling-off particles are locked in the concrete block, resulting in a small increase in the quality of concrete specimen when the ultrasonic velocity and compressive strength are reduced. However, there is a strong correlation between relative ultrasonic velocity factor and relative compressive strength factor, showing a linear relationship, and the correlation reliability is as high as 0.999. Ultrasonic nondestructive testing can be used to characterize the change of compressive strength, and the corresponding relationship is as follows.

FIGURE 3 | Corresponding relationship of three corrosion factors.

FIGURE 4 | SEM images of C50-0 concrete before and after sulfate corrosion.
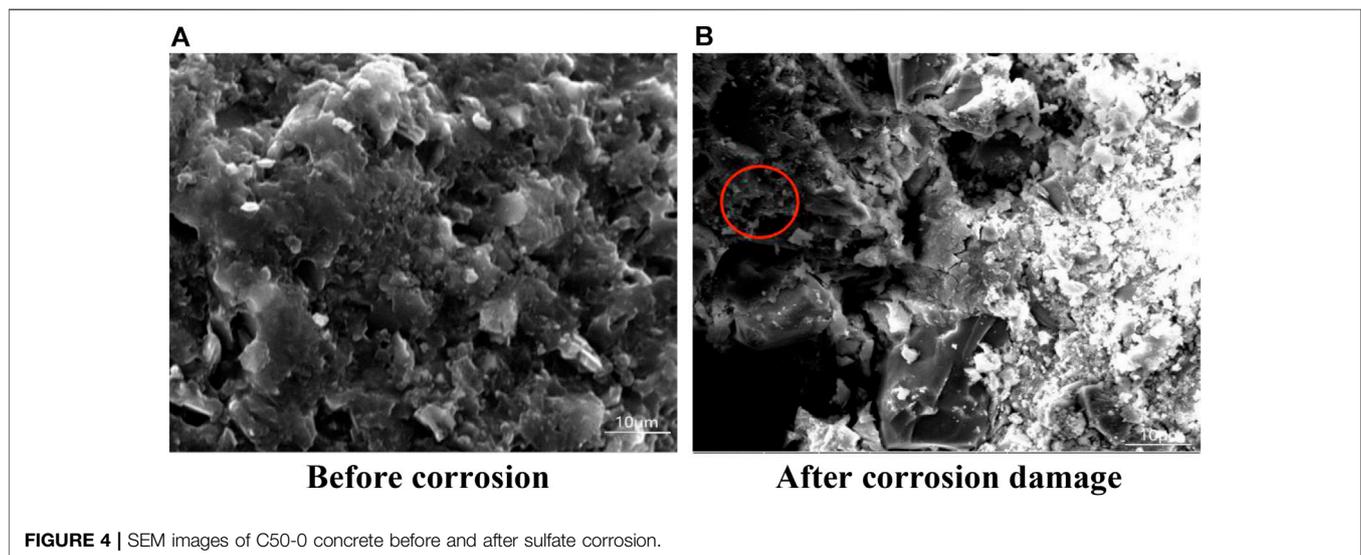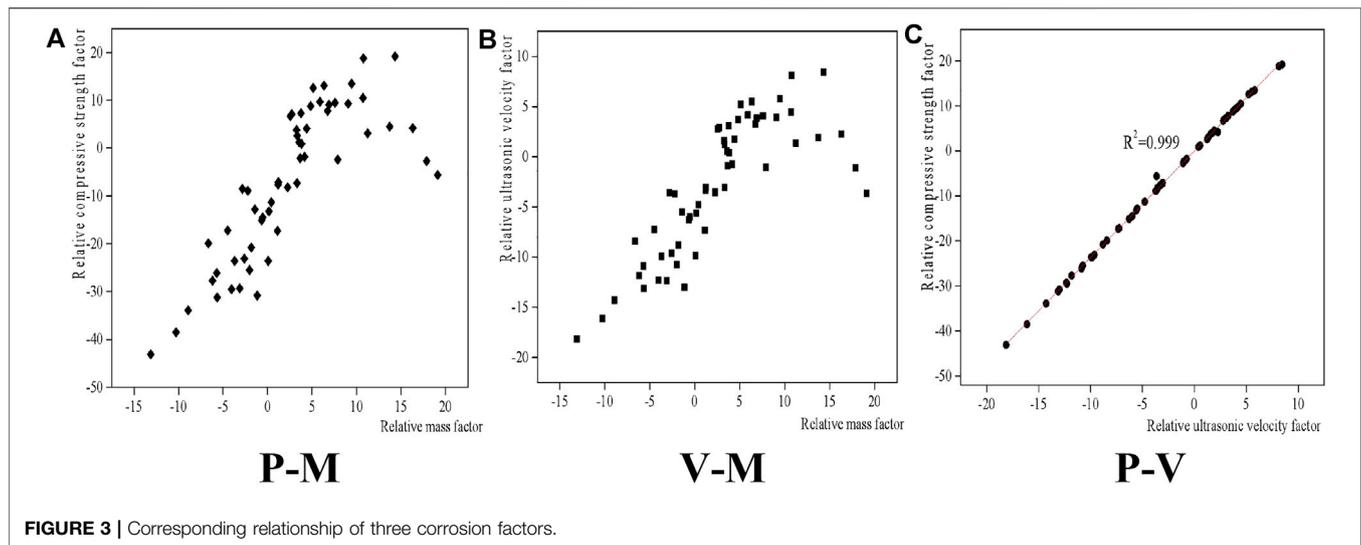
$$P = 2.365V - 0.0274$$

With the above formula, the concrete compressive strength can be converted by ultrasonic velocity, so as to understand the corrosion degree of concrete subjected to sulfate wetting–drying cycles.

## Sulfate Corrosion Deterioration Mechanism of Metal Tailings Powder Concrete

In order to explore the corrosion deterioration mechanism of metal tailings powder concrete after sulfate wetting–drying cycle, the C50-0 group with single slag powder and C50-50 group with strong sulfate corrosion resistance are selected to study the micro morphology and products of concrete before corrosion and after corrosion damage by SEM and XRD. **Figures 4** and **5** shows the

SEM image of concrete before and after corrosion. The image is of ×5,000 magnification.

Compared with the micro morphology of the concrete before and after corrosion, the internal structure of the concrete before corrosion is very dense. After sulfate wetting–drying cycle damage, there are many flake gypsum and some needle rod ettringite in the concrete. The volume of these corrosion products expands, the expansion stress is greater than the tensile stress in the concrete, and cracks appear in the concrete, resulting in the damage of the micro morphology. The macroscopic performance is that the compressive strength of concrete decreases to 75% of the initial strength.

Figure 6 is the XRD spectrum of concrete before and after the sulfate wetting–drying cycle corrosion damage. From the spectrum, excluding the influence of silica, there is an obvious $Ca(OH)_2$ diffraction peak before corrosion. But after corrosion

FIGURE 5 | SEM images of C50-50 concrete before and after sulfate corrosion.

FIGURE 6 | XRD spectrum of concrete before and after sulfate corrosion failure.
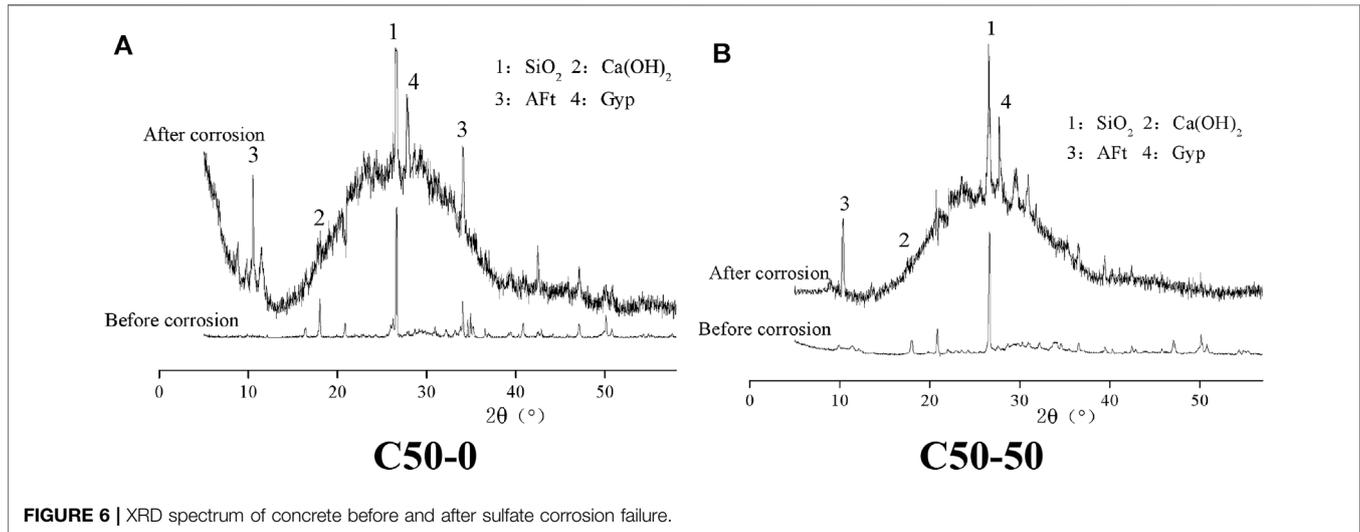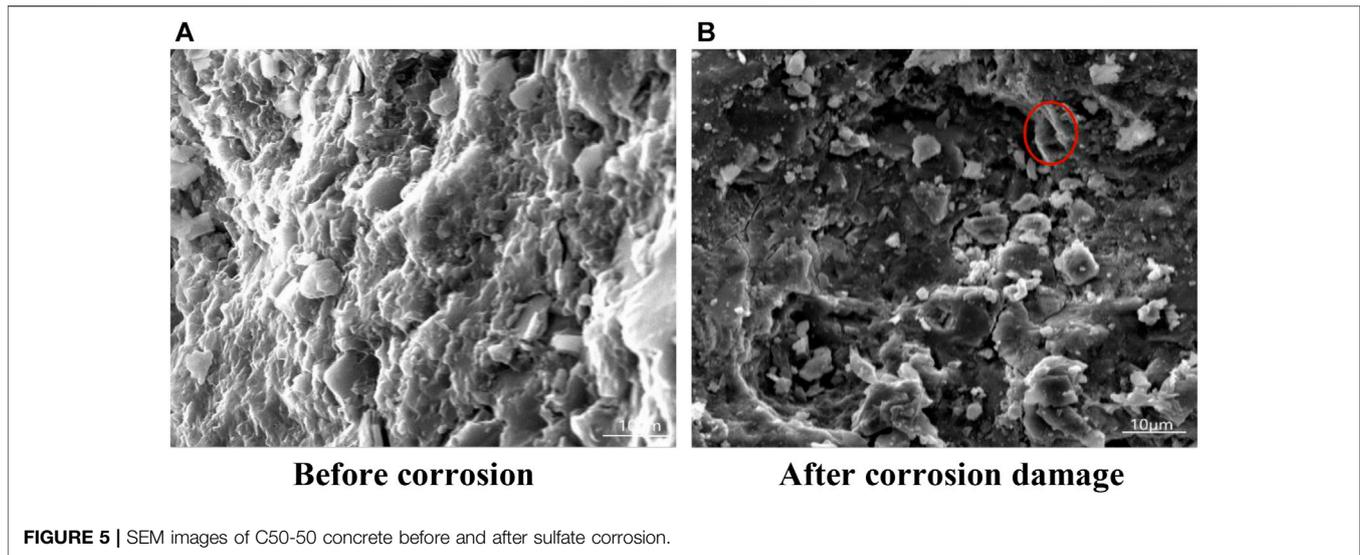
damage, the $Ca(OH)_2$ diffraction peak no longer exists. There are obvious ettringite and gypsum diffraction peaks after corrosion, which indicates that the sulfate corrosion of concrete is mainly due to the sodium sulfate solution entering the concrete and reacting with the internal $Ca(OH)_2$. The production reaction formula of ettringite is as follows:

$$Na_2SO_4 \cdot 10H_2O + Ca(OH)_2 \rightarrow CaSO_4 \cdot 2H_2O + 2NaOH$$
$$+ 8H_2O$$

$$3(CaSO_4 \cdot 2H_2O) + 4CaO \cdot Al_2O_3 \cdot 12H_2O + 14H_2O \rightarrow 3CaO$$
$$\cdot Al_2O_3 \cdot 3CaSO_4 \cdot 32H_2O + Ca(OH)_2$$
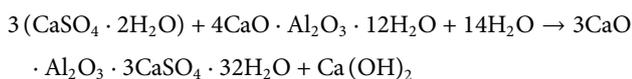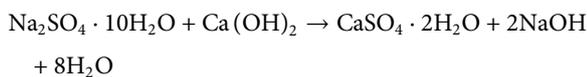
Gypsum formation reaction is as follows:
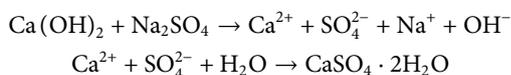
$$Ca(OH)_2 + Na_2SO_4 \rightarrow Ca^{2+} + SO_4^{2-} + Na^+ + OH^-$$
$$Ca^{2+} + SO_4^{2-} + H_2O \rightarrow CaSO_4 \cdot 2H_2O$$

Proper addition of metal tailings powder can increase the sulfate corrosion resistance of concrete. Combined with the analysis of SEM and XRD test results, the $Ca(OH)_2$ diffraction peak intensity of concrete with metal tailings powder accounting for 50% of mineral admixture before corrosion is significantly lower than that of the C50-0 group with slag powder alone. XRD analysis after corrosion shows that the diffraction peak intensity of ettringite and gypsum in the C50-50 group is significantly lower than that in the C50-0 group, which shows that the addition of metal tailings powder can effectively reduce the generation of sulfate corrosion products, so as to improve the ability of concrete to resist sulfate corrosion.

Nuclear magnetic resonance (NMR) is used to test the porosity of the two kinds of concrete, and the harmless holes (below 0.02 μm), less harmful holes (0.02–0.1 μm), harmful holes (0.1–0.2 μm), and multi harmful holes (above 0.2 μm) are

TABLE 9 | Porosity of concrete (%).

	Total porosity	Below 0.02 μm	0.02-0.1 μm	0.1-0.2 μm	Above 0.2 μm
C50-0	7.12	6.64	0.21	0.11	0.16
C50-50	7.59	6.83	0.58	0.09	0.09

calculated, as shown in **Table 9**. It can be found that the addition of metal tailings powder will increase the number of less harmful holes and harmless holes in concrete. The introduction of these holes can effectively reduce the stress formed by the expansion of sulfate corrosion products and improve the ability of concrete to resist sulfate corrosion.

The results show that an appropriate amount of inactive metal tailings powder can reduce the content of $Ca(OH)_2$ in concrete, so as to reduce the formation of ettringite, gypsum, and other corrosion products. At the same time, the metal tailings powder will optimize the pore structure and reduce the expansion stress of corrosion products.

CONCLUSION

(1) The sulfate resistance of C30 concrete has no strong correlation with the metal tailings powder content, and the sulfate resistance grade is KS120. Proper addition of metal tailings powder can increase the sulfate resistance of C50 concrete, which can reach more than KS150. When the content of metal tailings powder and slag powder is 3:7 and 5:5, the sulfate resistance of C50 concrete is the strongest, up to KS180.

(2) There is a linear relationship between relative ultrasonic velocity factor and relative compressive strength factor. Nondestructive ultrasonic testing can be used to reflect the compressive strength of concrete after a certain number of wetting–drying and cycles.

(3) By analyzing the microscopic test results of concrete such as SEM, XRD, and NMR, the sulfate damage mechanism of metal tailings powder concrete is mainly the internal generation of corrosion products ettringite and gypsum. The introduction of metal tailings powder can reduce the concrete alkalinity and improve the pore structure, so as to improve the sulfate corrosion resistance of concrete.

DATA AVAILABILITY STATEMENT

The original contributions presented in the study are included in the article/Supplementary Material, further inquiries can be directed to the corresponding author.

AUTHOR CONTRIBUTIONS

JL and RW conceived and designed the experiments; RW, MZ, GZ, and YZ performed the experiments; RW and JL wrote the paper. All authors read and approved the manuscript.

FUNDING

REFERENCES

Chen, Q., Tao, Y., Zhang, Q., and Qi, C. (2022). The Rheological, Mechanical and Heavy Metal Leaching Properties of Cemented Paste Backfill under the Influence of Anionic Polyacrylamide. *Chemosphere* 286, 131630. doi:10.1016/j.chemosphere.2021.131630

Han, F., Li, L., Song, S., and Liu, J. (2017). Early-age Hydration Characteristics of Composite Binder Containing Iron Tailing Powder. *Powder Technol.* 315, 322–331. doi:10.1016/j.powtec.2017.04.022

Han, F., Song, S., Liu, J., and Huang, S. (2019). Properties of Steam-Cured Precast concrete Containing Iron Tailing Powder. *Powder Technol.* 345, 292–299. doi:10.1016/j.powtec.2019.01.007

Hou, Y. F., Liu, J. T., Zhao, S. R., and Peng, X. D. (2019). Effect Mechaniam of Iron Tailing Powder on Cement Mortar Properties. *Joural Basic Sci. Eng.* 27 (05), 1149–1157. doi:10.16058/j.issn.1005-0930.2019.05.018

Huang, T. M., Li, S. C., Li, X. H., Zhang, P. J., Yang, H. B., Ruan, L., et al. (2021). Study on Resource Utilization Technology of Nonferrous Metals Tungsten and lead-zinc Tailings. *Chin. J. Nonferrous Met.* 31 (4), 1057–1073. doi:10.11817/j.ysxb.1004.0609.2021-39637

Li, N., Lv, S. W., Wang, W., Guo, J., Jiang, P., and Liu, Y. (2021). Experimental Investigations on the Mechanical Behavior of Iron Tailings Powder with Compound Admixture of Cement and Nano-clay. *Construction Building Mater.* 254, 119259. doi:10.1016/j.conbuildmat.2020.119259

Liu, J.-h., Zhou, Y.-c., Wu, A.-x., and Wang, H.-j. (2019). Reconstruction of Broken Si-O-Si Bonds in Iron Ore Tailings (IOTs) in concrete. *Int. J. Miner Metall. Mater.* 26 (10), 1329–1336. doi:10.1007/s12613-019-1811-z

Liu, J. H., Wu, R. D., Wu, A. X., and Wang, S. Y. (2017). Bleeding Characteristics and Improving Mechanism of Self-Flowing Tailings Filling Slurry with Low Concentration. *Minerals* 7 (8), 1–7. doi:10.3390/min7080131

Lu, D., Zhong, J., Yan, B., Gong, J., He, Z., Zhang, G., et al. (2021). Effects of Curing Conditions on the MECHANICAL and Microstructural Properties of Ultra-high-performance Concrete (UHPC) Incorporating Iron Tailing Powder. *Materials* 14 (1), 215. doi:10.3390/ma14010215

Lvu, X. D., Liu, Z. A., Zhu, Z. G., and Li, B. X. (2018). Study of the Progress of Tailings Comprehensive Utilization of Raw Materials in Cement and concrete. *Mater. Rep.* 32 (S2), 452–456.

Qi, C., and Fourie, A. (2019). Cemented Paste Backfill for mineral Tailings Management: Review and Future Perspectives. *Minerals Eng.* 144, 106025. doi:10.1016/j.mineng.2019.106025

Ruidong, W., Yu, S., Juanhong, L., Linian, C., Guangtian, Z., and Yueyue, Z. (2021). Effect of Iron Tailings and Slag Powders on Workability and Mechanical Properties of concrete. *Front. Mater.* 8, 723119. doi:10.3389/fmats.2021.723119

Song, S. M., and Chen, H. Y. (2020). Influence of Iron Tailings Powder on Performance of Low Clinker Cementitious Material concrete. *Bull. Chin. Ceram. Soc.* 39 (08), 2557–2566. doi:10.16552/j.cnki.issn1001-1625.2020.08.026

Song, S. M., and Liu, X. D. (2017). Lnfluence of Iron Ore Tailings Powder on the Performance of High Fluidity concrete. *Concrete* 11, 77–80. doi:10.3969/j.issn.1002-3550.2017.11.018

Song, S. M., Zhang, L. Y., and Li, Z. Y. (2019). Effect of Iron Tailings Micropowder on Late-Property of Cement concrete. *Concrete* 01, 128–131. doi:10.3969/j.issn.1002-3550.2019.01.031

Ullah, S., Yang, C., Cao, L., Wang, P., Chai, Q., Li, Y., et al. (2021). Material Design and Performance Improvement of Conductive Asphalt concrete Incorporating Carbon Fiber and Iron Tailings. *Construction Building Mater.* 303, 124446. doi:10.1016/j.conbuildmat.2021.124446

Wu, D., Cai, S.-j., and Huang, G. (2014). Coupled Effect of Cement Hydration and Temperature on Rheological Properties of Fresh Cemented Tailings Backfill Slurry. *Trans. Nonferrous Met. Soc. China* 24 (9), 2954–2963. doi:10.1016/S1003-6326(14)63431-2

Wu, R., and Liu, J. (2018). Experimental Study on the concrete with Compound Admixture of Iron Tailings and Slag Powder under Low Cement Clinker System. *Adv. Mater. Sci. Eng.* 2018, 1–7. doi:10.1155/2018/9816923

Wu, R., Liu, J., Zhang, G., Zhang, Y., and An, S. (2020). Research on Carbonation Characteristics and Frost Resistance of Iron Tailings Powder concrete under Low-Cement Clinker System. *Adv. Mater. Sci. Eng.* 2020, 1–11. doi:10.1155/2020/9192757

Yang, H. M., and Guo, J. L. (2018). *Tailings and Waste Rock Comprehensive Utilization technology[M]*. Beijing: Chemical Industry Press, 187–217. doi:10.1016/b978-0-12-803581-8.10303-0

Yang, J., Xu, L.-h., Wu, H.-q., and Jin, J. (2021). Preparation and Properties of Porous Ceramics from Spodumene Flotation Tailings by Low-Temperature Sintering. *Trans. Nonferrous Met. Soc. China* 31 (9), 2797–2811. doi:10.1016/S1003-6326(21)65694-7

Yao, H. H., Cai, L. B., Liu, W., Qin, W. Q., Jiao, F., and Yang, C. R. (2021). Current Status and Development of Comprehensive Utilization of Waste Rock in Metal Mines in China. *Chin. J. Nonferrous Met.* 31 (6), 1649–1660. doi:10.11817/j.ysxb.1004.0609.2021-35986

Zhang, N., Tang, B., and Liu, X. (2021). Cementitious Activity of Iron Ore Tailing and its Utilization in Cementitious Materials, Bricks and concrete. *Construction Building Mater.* 288, 123022. doi:10.1016/j.conbuildmat.2021.123022

Zhang, P. J., Huang, T. M., He, H. J., Wei, X. X., Zhao, M. M., Ruan, L., et al. (2019). Hydrothermal Synthesis of ZSM-5 Using Tin Ore Tailing as Raw Material. *Chin. J. Nonferrous Met.* 29 (08), 1790–1800. doi:10.19476/j.ysxb.1004.0609.2019.08.24

Zhang, Q.-l., Li, Y.-t., Chen, Q.-s., Liu, Y.-k., Feng, Y., and Wang, D.-l. (2021). Effects of Temperatures and pH Values on Rheological Properties of Cemented Paste Backfill. *J. Cent. South. Univ.* 28 (6), 1707–1723. doi:10.1007/s11771-021-4728-4

Zhao, Y., Zhao, G. Y., Pei, D. F., Wu, P., Qiu, J., and Li, Y. (2021). Analysis on Connotation, Characteristics and Type of green Mining Mode for Underground Metal Mines. *Chin. J. Nonferrous Met.* doi:10.11817/j.ysxb.1004.0609.2021-40152